

# Granular Flows

J. Goddard

*University of California San Diego*

## 1 Introduction

Granular materials represent a major object of human activities: as measured in tons, the first material manipulated on earth is water; the second is granular matter. . . This may show up in very different forms: rice, corn, powders for construction. . . In our supposedly modern age, we are extraordinarily clumsy with granular systems. . .

P. G. de Gennes, “From Rice to Snow”, Nishina Memorial Lectures, 2008

The epigrammatic quote by a French Nobel laureate is familiar to many in the field of granular mechanics and reflects a long-standing scientific fascination and practical interest. This is acknowledged by many others and summarized in the articles listed under Further Reading.

As a general definition, we understand by *granular medium* a particle assembly dominated by pairwise nearest-neighbor interactions and usually limited to particles larger than 1 micrometer in diameter, for which the direct mechanical effects of Van der Waals and ordinary thermal (“Brownian”) forces are negligible. This includes a large class of materials, such as cereal grains, pharmaceutical tablets and capsules, geomaterials such as sand, and the masses of rock and ice in planetary rings.

Most of the present article is concerned with dry granular materials in which there are negligible effects of air or other gases in the interstitial space, or else with granular materials completely saturated by an interstitial liquid. In this case, liquid surface-tension at “capillary necks” between grains, as in the wet sand of sand castles, or related forms of cohesion are largely negligible.

There are several important and interrelated aspects of granular mechanics: (i) experiment and industrial or geotechnical applications, (ii) analytical and computational micromechanics (grain-level dynamics), (iii) homogenization (“upscaling” or “coarse graining”) to obtain smoothed

continuum models from the Newtonian mechanics of discrete grains, (iv) mathematical classification and solution of the continuum field equations for granular flow, and (v) development of continuum models (“constitutive equations”) for stress-deformation behavior. The present article focuses on (v), since the study of most of the preceding items either depends on it, or is strongly motivated by it. The following discussion of (iv) sets the stage for the subsequent coverage of (v).

## 2 Field Equations and Constitutive Equations

By *field equations*, we mean the partial differential equations (PDEs), with time  $t$  and spatial position  $\mathbf{x} \doteq [x_i]$  as independent variables, that represent the continuum-level mass and linear momentum balances governing the density  $\rho(\mathbf{x}, t)$ , velocity  $\mathbf{v}(\mathbf{x}, t) \doteq [v_i]$ , and symmetric stress tensor  $\mathbf{T}(\mathbf{x}, t) \doteq [\tau_{ij}]$ , for any material,

$$\dot{\rho} = -\rho \nabla \cdot \mathbf{v} \quad \text{and} \quad \rho \dot{\mathbf{v}} = \nabla \cdot \mathbf{T}. \quad (1)$$

The indices refer to components in Cartesian coordinates, and the notation “ $\doteq [ ]$ ” indicates components of vectors and tensors in those coordinates. Written out, (1) becomes  $\partial_t \rho + \partial_j (\rho v_j) = 0$  and  $\partial_t (\rho v_i) = \partial_j (\tau_{ij} - \rho v_i v_j)$  for  $i = 1, 2, 3$ , where  $\dot{w} = \partial_t w + v_j \partial_j w$  for any quantity  $w$ , sums from  $j = 1$  to 3 are taken over terms with repeated indices,  $\partial_i w = \partial w / \partial x_i$ ,  $\partial_t w = \partial w / \partial t$ , and the product rule has been used. For more information on (1), see CONTINUUM MECHANICS [4.X].

There are ten dependent variables,  $\rho$ ,  $v_i$ , and  $\tau_{ij} = \tau_{ji}$ , but only four equations in (1). In order to “close” them (to make them soluble), we need six more equations. For example, the closure representing the constitutive equations for an incompressible Newtonian fluid (see NAVIER–STOKES EQUATIONS [3.X]) is

$$\mathbf{T}' = 2\eta \mathbf{D}' \quad \text{and} \quad \rho = \text{constant}, \quad (2)$$

where  $\eta$  is a coefficient of shear viscosity and  $\mathbf{D}$  denotes the *rate of deformation*, also a symmetric second-rank tensor,  $\mathbf{D} = \text{sym } \nabla \mathbf{v} \doteq \frac{1}{2} [\partial_i v_j + \partial_j v_i]$ , where “sym” denotes the symmetric part of a second-rank tensor and the prime denotes the *deviator* (“traceless” or “shearing” part),  $\mathbf{X}' =$

$\mathbf{X} - \frac{1}{3}(\text{tr } \mathbf{X})\mathbf{I}$ ,  $X'_{ij} = X_{ij} - \frac{1}{3}X_{kk}\delta_{ij}$ , where  $\delta_{ij}$  are the components of the identity  $\mathbf{I}$ .

For rheologically more complicated (“complex”) fluids, such as *viscoelastic liquids*, the stress at a material point may depend on the entire past history of the velocity gradient  $\nabla\mathbf{v}$  at that point. Viscoelasticity is exemplified by the simplest form of the *Maxwell fluid* giving the rate of change of  $\mathbf{T}'$  as a linear function of  $\mathbf{D}'$  and  $\mathbf{T}'$ ,

$$\overset{\circ}{\mathbf{T}}' = 2\mu\mathbf{D}' - \lambda\mathbf{T}' = \lambda(2\eta\mathbf{D}' - \mathbf{T}'), \quad (3)$$

where  $\overset{\circ}{\mathbf{X}} = \dot{\mathbf{X}} + \text{sym}(\mathbf{X}\mathbf{W})$ ,  $\mathbf{X}\mathbf{W} \hat{=} [X_{ik}W_{kj}]$ ,  $\mathbf{W}$  is the skew part of the velocity gradient,  $\mathbf{W} \hat{=} \frac{1}{2}[\partial_i v_j - \partial_j v_i]$ ,  $\lambda$  is the *relaxation rate* or inverse of the *relaxation time*, and  $\mu$  is the elastic modulus. In this simple model,  $\mu$  can be identified with the elastic shear modulus  $G$  to be discussed below.

According to (3), which was proposed in a slightly different form by the famous physicist James Clerk Maxwell in 1867, the coefficient of viscosity and the elastic modulus are connected by  $\eta = \mu/\lambda$ , and a material responds elastically on a time scale  $\lambda^{-1}$  with viscosity and viscous dissipation arising from relaxing elastic stress.

One obtains from (3) elastic-solid or visco-fluid behavior in the respective limits  $\lambda \rightarrow 0$  or  $\lambda \rightarrow \infty$ . This is illustrated by the quintessential viscoelastic material “silly putty” which bounces elastically but undergoes viscous flow in slow deformations. Rheologists employ a *Deborah number* of the form  $\dot{\gamma}/\lambda$  to distinguish between rapid, solid-like and slow fluid-like deformations.

The superposed “o” in (3) denotes a *Jaumann derivative*, which gives the time rate of change in a frame translating with a material point and rotating with the local material spin. The Jaumann derivative is the simplest *objective* time derivative that embodies the *principle of material frame indifference*. This principle, which is not a fundamental law of mechanics, is tantamount to the assumption that arbitrary rigid-body rotations superimposed on a given motion of a material merely rotate stresses in the same way. Stated more generally, accelerations of a body relative to an inertial (“Newtonian”) frame do not affect the stress-deformation behavior. The principle is already reflected in the simpler constitutive equa-

tion (2), where only the symmetric part of  $\nabla\mathbf{v}$  is allowed.

While frame-indifference is a safe assumption for most molecular materials, which are dominated at the molecular level by random thermal motion, it could conceivably break down for granular flows, where random granular motions are comparable to those associated with macroscopic shearing. Nevertheless, the assumption will be adopted in the constitutive models considered here.

Note that, for a fixed material particle  $\mathbf{x}^\circ$ , (3) represents a set of five simultaneous ordinary differential equations, which we call *Lagrangian ordinary differential equations* (LODEs). In the *Eulerian* or spatial description, they must be combined with (1) to provide nine equations in the nine dependent variables,  $p = -\frac{1}{3}\text{tr } \mathbf{T}$ ,  $\mathbf{v}$  and  $\mathbf{T}'$ , governing the velocity field of the Maxwell fluid. The solution, subject to various initial and boundary conditions, is no easy task and usually requires advanced numerical methods.

We identify below a broad class of plausible constitutive equations, which basically amount to generalizations of (3), and include the so-called *hypoplastic* models for granular plasticity. It turns out that all these can be obtained from elastic and inelastic potentials, which are familiar in classical theories of elastoplasticity. The above models can be enlarged to include models of visco-elastoplasticity that are broadly applicable to all the prominent regimes of granular flow. Following the brief review in the following section of phenomenology and flow regimes, a systematic outline of the genesis of such models will be presented.

The present article does not cover a large body of literature dealing with numerical methods, neither the direct simulation of micromechanics by the distinct element method (DEM), nor solution of the continuum field equations based on finite element methods (FEM) or related techniques.

### 3 Phenomenological Aspects

We consider here the important physical parameters and dimensionless groups that characterize the various regimes of granular mechanics and flows. The review article of Forterre and

Pouliquen provides more quantitative comparisons for fairly simple shearing flows.

### Key parameters and dimensionless groups

Apart from various dimensionless parameters describing grain shape, the most prominent physical parameters for non-cohesive granular media are: grain elastic (shear) modulus  $G_s$ , intrinsic grain density  $\rho_s$ , representative grain diameter  $d$ , intergranular (Coulomb) contact-friction coefficient  $\mu_s$  or macroscopic counterpart  $\mu_C$ , and confining pressure  $p_s$ . These parameters define the key dimensionless groups that serve to delineate various regimes of granular flow, namely an *elasticity number*, an *inertia number*, and a *viscosity number*, given respectively by

$$\mathbb{E} = G_s/p_s, \quad \mathbb{I} = \dot{\gamma}d\sqrt{\rho_s/p_s}, \quad \mathbb{H} = \eta_s\dot{\gamma}/p_s,$$

and involving  $\dot{\gamma}$ , a representative value of the shear rate  $|\mathbf{D}'|$ . In addition, we will have occasion to refer briefly below to a Knudsen number based on the ratio of microscopic to macroscopic length scales.

Note that  $\mathbb{I}$  is the analog of the Deborah number mentioned above, but now involving a relaxation rate that represents the competition between grain inertia and Coulomb friction  $\mu_C p_s$ . The quantity  $\mathbb{I}^2$  represents the ratio of representative granular kinetic energy  $\rho_s d^2 \dot{\gamma}^2$  to frictional confinement.

The transition from a fluid-saturated granular medium to a dense fluid-particle suspension occurs when the viscosity number  $\mathbb{H} \approx 1$ , where viscous and frictional contact forces are comparable.

In the case of fluid-particle suspensions, it is customary to identify  $\mathbb{I}^2/\mathbb{H}$  as the ‘‘Stokes number’’ or the ‘‘Bagnold number’’ (after a pioneer in granular flow) representing the magnitude of grain-inertial to viscous forces.

In the following sections, we shall focus attention on dry granular media, including later only the briefest mention of fluid-particle systems.

### Granular flow regimes

Although granular materials are devoid of intrinsic thermal motion at the grain level, they nevertheless exhibit states that resemble the solid, liq-

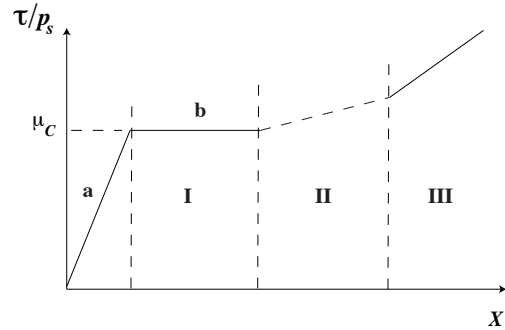


Figure 1: Schematic diagram of granular-flow regimes

uid and gaseous states of molecular systems. All these granular states may co-exist in the same flow field, as the analogs of ‘‘multiphase flow.’’ There are several open questions as to the proper matching of solid-like immobile states with the rapidly sheared states that cannot be addressed in this brief article.

With  $\tau$  denoting a representative shear stress and  $\gamma$  a representative shear strain relative to a rest state (in which  $\tau/p_s = 0$  and  $\mathbb{I} = 0$ ), the various flow regimes are shown in the qualitative, highly simplified sketch in Fig. 1, and in Table 1. In Fig. 1, the dimensionless ratio  $\tau/p_s$  is represented as a function of a single dimensionless variable representing an interpolating form,

$$X \sim \mu_C \mathbb{E} \gamma / (\mathbb{E} \gamma + \mu_C) + \mathbb{I}^2. \quad (4)$$

(A compound representation, closer to the constitutive models considered below and illustrated in Fig. 5, is  $\tau/p_s = \mu_C + \mathbb{I}^2$  with  $\gamma_E = (\tau/p_s)\mathbb{E}$ , where the first of these represents a Coulomb–Bagnold interpolation found in certain constitutive models and  $\gamma_E$  is elastic deformation at any stress state.)

Figure 1 fails to capture the strong nonlinearity and history-dependence of granular plasticity in regime Ib, a matter addressed by the constitutive models to be discussed below.

Like the liquid states of molecular systems, dense-rapid flow, represented as a general dimensionless function  $f(\mathbb{I})$  in Table 1, may be the most poorly understood regime of granular mechanics. It involves important phenomena such as the fascinating granular size-segregation. There is some

Table 1: Granular-flow regimes in Fig. 1. The last column gives the scaling of the stress  $\tau$

I.	Quasi-static: (Hertz–Coulomb) elastoplastic “solid”	
Ia.	(Hertz) elastic	$G_s \gamma$
Ib.	(Coulomb) elastoplastic	$\mu_C$
II.	Dense-rapid: viscoplastic “liquid”	$p_s f(\mathbb{I})$
III.	Rarified-rapid: (Bagnold) viscous “granular gas”	$\rho_s d^2 \dot{\gamma}^2$

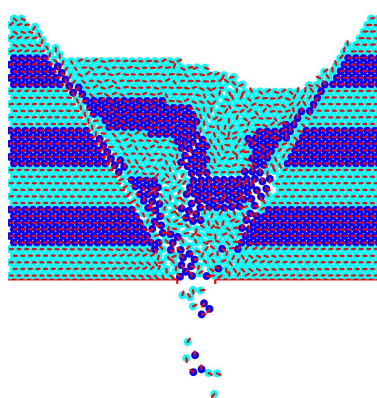
evidence that this regime may involve an additional dependence on  $\mathbb{E}$  for soft granular materials.

**The elastic regime.** The geometry of contact between quasi-spherical linear (Hookean) elastic particles should lead to nonlinear elasticity of a granular mass at low confining pressures  $p_s$  and to an interesting scaling of elastic moduli and elastic wave speeds with pressure.

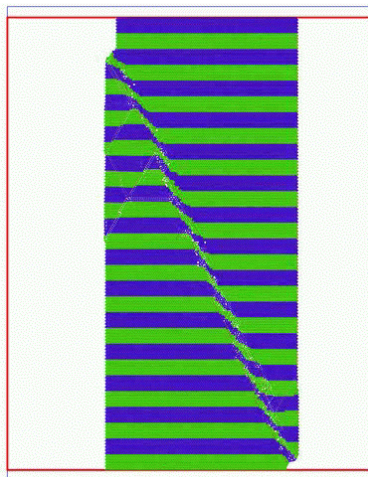
Based on Hertzian contact mechanics, a rough “mean-field” estimate of the continuum shear modulus  $G$  in terms of grain shear modulus  $G_s$  is given by  $G/G_s \sim \mathbb{E}^{-1/3}$ , which indicates a  $\frac{1}{3}$ -power dependence on pressure. For example, with  $p_s \sim 100$  kPa and  $G_s \sim 100$  GPa (a rather stiff geomaterial), one finds  $\mathbb{E} \sim 10^6$  and  $G \sim 10^{-2} G_s$ , amounting to a huge reduction of global stiffness due to relatively soft Hertzian contact.

In principle, we should replace  $G_s$  by  $G$  in Table 1 and (4), and  $\mathbb{E} = G_s/p_s$  by  $G/p_s = \mathbb{E}^{-2/3}$ . In so doing, we obtain an estimate of the limiting elastic strain for the onset of Coulomb slip (with  $\mu_C \sim 1$ ) to be  $\gamma_E \sim \mathbb{E}^{-2/3} \sim 10^{-4}$ , given the above numerical value. Although crude, this provides a reasonable estimate of the small elastic range of stiff geomaterials such as sand.

**The elastoplastic regime.** Given its venerable history, dating back to the classical works of Coulomb, Rankine, and others in the 18th and 19th centuries, and its enduring relevance to geomechanics, the field of elastoplasticity is the most thoroughly studied area of granular me-



(a) Shear bands in slow hopper flow

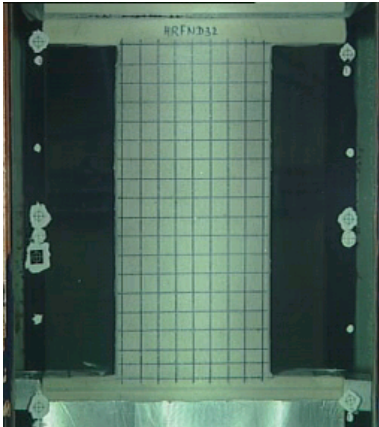


(b) Shear bands in axial compression

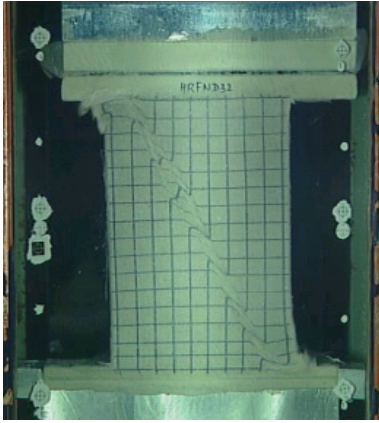
Figure 2: DEM simulations (Courtesy of W. Ehlers)

chanics. Here, we touch on a few salient phenomena and the theoretical issues surrounding them, as background for the discussion of constitutive modeling to follow.

Figure 2 shows the results from the 2D DEM simulations of Prof. W. Ehlers (University of Stuttgart) of a quasi-static hopper discharge and a biaxial compression test, both of which illustrate a well-known localization of deformation into shear bands. A hallmark of granular plasticity, this localized slip (or “failure”) may be implicated in dynamic “arching,” with large transient stresses on bounding surfaces such as hopper walls or structural retaining walls. Similar phenomena are implicated in large-scale landslides.



(a) Before compression



(b) After compression

Figure 3: Experimental axial compression of dry Hos-tun sand specimen (Courtesy of W. Ehlers)

Figure 3 shows the development of shear bands in a standard experimental quasi-static compression test on a sand column surrounded by a thin elastic membrane. The literature abounds with many interesting experimental observations and numerical simulations; see, e.g., Tejchman’s book.

The occurrence of shear bands can be viewed mathematically as material *bifurcation and instability* arising from loss of convexity in the underlying constitutive equations, accompanied by a *change of type* in the PDEs involved in the field equations. We recall that similar changes of type, e.g., from elliptic to hyperbolic PDEs, are associated with phenomena such as the gas dynamic transition from subsonic to supersonic flows with formation of thin “shocks.”

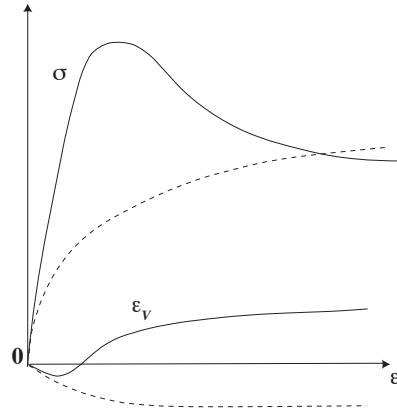


Figure 4: Schematic diagram of triaxial stress/dilatation-strain curves for initially dense (solid curves) and loose (dashed curves) sands

To help understand the elastoplastic instability, Fig. 4 presents a qualitative sketch of the typical stress-strain/dilatancy behavior in the axial compression of dense and loose sands, with  $\sigma$  denoting compressive stress,  $\varepsilon$  compressive strain, and  $\varepsilon_V = \log(V/V_0)$  volumetric strain (where a volume  $V_0$  has been deformed into  $V$ ). While no numerical scale is shown on the axes, the peak stress and the change of  $\varepsilon_V$  from negative (contraction) to positive (dilation) typically occur at strains of the order of few percent ( $\varepsilon \sim 0.01\text{--}0.05$ ) for dense sands.

Although tempting to regard the initial growth of  $\sigma$  with  $\varepsilon$  as elastic in nature, the elastic regime is represented by much smaller strains (corresponding to the estimates of order  $10^{-4}$  given above), corresponding to a nearly vertical unloading from any point on the  $\sigma$ - $\varepsilon$  curve. It is therefore much more plausible that the initial stress growth represents an *almost completely dissipative* plastic “hardening” associated with compaction ( $\varepsilon_V < 0$ ) accompanied by growth of contact number density  $n_c$  and contact anisotropy, whereas the maximum in stress can be attributed to the subsequent decrease in  $n_c$  accompanying dilation ( $\varepsilon_V > 0$ ).

As will be discussed below, one can rationalize the formation of shear bands as the result of “strain softening” or unstable “wrong-way” be-

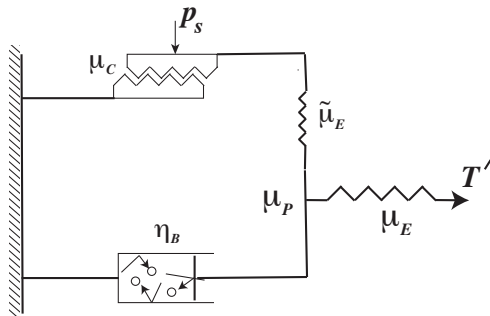


Figure 5: Slide-block/spring/dashpot analog of visco-elastoplasticity

havior (decrease of incremental force with incremental displacement) following the peak stress. According to certain analyses, this can arise as a purely dissipative process associated with the decrease of plastic stress, whereas according to others it may result from a peculiar quasi-elastic response.

Whatever the precise nature of the material instability, it generally calls for *multipolar* or “higher-gradient” constitutive models involving an intrinsic material length scale. Hence, to our list of important dimensionless parameters we must now add a *Knudsen number*  $\mathbb{K} = \ell/L$  as discussed further below. Suffice it to say here that a material length scale  $\ell$  is necessary to *regularize* field equations in order to avoid sharp discontinuities in strain rate by assigning finite thickness to zones of strain localization. Such a scale, clearly evident in the DEM simulations and experiments of Figs. 2 and 3, cannot be predicted with the *non-polar* models that constitute the main subject of this article.

**Springs and slideblocks.** Setting aside length-scale effects, the simple mechanical model in Fig. 5 provides a useful intuitive view of the continuum model considered below. There, the applied force  $\mathbf{T}'$  is the analog of continuum-mechanical shear stress, and the rate of extension of the device represents deviatoric deformation rate  $\mathbf{D}'$ .

The serrated slide-block at the top of Fig. 5 is a modification of the standard flat plastic slide-block, where sliding stress  $\tau$  represents a pressure independent yield stress, or a frictional slide-block with  $\tau/p_s = \mu_C$  representing the (Amontons–Coulomb) coefficient of sliding friction. The serrated version represents the granular “interlocking” model of Taylor (1948) or the “sawtooth” model of Rowe (1962) based on the concept of granular *dilatancy* introduced in 1885 by Osborne Reynolds (who is also renowned for his work in various fields of fluid mechanics). According to Reynolds the shearing resistance of a granular medium is partly due to volumetric expansion against the confining pressure. Thus, if the sawtooth angle vanishes, then one obtains a standard model of plasticity, with resistance due solely to yield stress or pressure-dependent friction.

At the point of sliding instability in the model, where the maximum volume expansion occurs, part of the stored volumetric energy must be dissipated by subsequent collapse and collisional impact. This may be assumed to occur on extremely short time scales giving rise to an apparent sliding friction coefficient  $\mu_C$  even if there is no sliding friction between grains ( $\mu_s = 0$ ). This rapid energy dissipation is emblematic of tribological and plastic-flow processes, where, owing to topological roughness and instability *in the small*, stored energy is thermalized on negligibly small time scales giving rise to rate-independent forces *in the large*.

As a second special feature of the model, the spring with constant  $\tilde{\mu}_E$  converts plastic deformation into “frozen elastic energy” and also provides an elementary model of plastic work hardening. It is intended to illustrate the fact that some of the stored elastic energy can never be entirely recovered solely by the mechanical action of  $\mathbf{T}'$ , which leads to history effects and associated complications in the thermodynamic theories of plasticity.

**Viscoplasticity.** For rapid granular flow, the viscous dashpot with (Bagnold) viscosity  $\eta_B$  (see Fig. 5) adds a rate-dependent force associated with granular kinetic energy and collisional dissipation. This leads to a form of *Bingham plas-*

*ticity* discussed below and described by certain rheological models, providing a rough interpolation between regimes I and III in Fig. 1. The viscous dashpot can also represent the effects of interstitial fluids. Note that removal of the plastic slide block gives the Maxwell model of viscoelasticity (3) whenever the spring and dashpot are linear.

Apart from presenting constitutive models that encompass those currently employed, we do not deal directly with the numerous issues and challenges in modeling the dense-rapid flow regime.

## 4 Constitutive Models

Inevitably, constitutive models for granular flow are complicated because of the wide range of phenomenology observed. We use a class of models that relate Cauchy stress  $\mathbf{T}$  to deformation rate  $\mathbf{D}$ , often referred to as the *Eulerian description*. In particular, we focus on a class of generalized *hypoplastic* models, based on a stress-space description that allows for nonlinear functions of stress. Although the approximation of linear elasticity is suitable for many granular materials, particularly stiff geomaterials, the nonlinear theory may find application to soft granular materials such as pharmaceutical capsules and clayey soils.

### Hypoplasticity

Let us start with an isotropic nonlinearly elastic material. This is one for which the stress  $\mathbf{T}$  and the finite (Eulerian) strain tensor  $\mathbf{E} = \frac{1}{2}(\mathbf{F}\mathbf{F}^T - \mathbf{I})$  are connected by isotropic relations of the form

$$\mathbf{T} = \mathbf{t}(\mathbf{E}) \quad \text{or} \quad \mathbf{E} = \mathbf{t}^{-1}(\mathbf{T}). \quad (5)$$

Here,  $\mathbf{F} = \partial\mathbf{x}/\partial\mathbf{x}^\circ$ , where  $\mathbf{x}^\circ$  and  $\mathbf{x}(\mathbf{x}^\circ)$  denote reference position and current placement, respectively, of material points. *Hyperelasticity* (or “Green elasticity”) is based on the thermodynamic consistency condition that the functions in (5) be derivable from elastic potentials. Truesdell’s *hypoelasticity*, a generalization of elasticity that allows for a more general rate-independent but path-dependent relation between stress and strain, is represented by the LODE

$$\overset{\circ}{\mathbf{T}} = \boldsymbol{\mu}_E(\mathbf{T}) : \mathbf{D}, \quad (6)$$

where  $\boldsymbol{\mu}_E$  is the fourth-rank hypoelastic modulus. With suitable integrability conditions on this modulus, it is possible to show that (6) implies an elastic relation of the form (5).

To obtain *visco-elastoplasticity* from (6), we adapt the *first fundamental postulate* of incremental plasticity, that the deformation rate can be decomposed into elastic and inelastic (or “plasticoviscous”) parts,  $\mathbf{D} = \mathbf{D}_E + \mathbf{D}_P$ . Then replace  $\mathbf{D}$  in the relations above by  $\mathbf{D}_E = \mathbf{D} - \mathbf{D}_P$  and provide a constitutive equation for  $\mathbf{D}_P$ .

As the *second fundamental postulate*, we assume that the elastic stress  $\mathbf{T}$  conjugate to  $\mathbf{D}_E$  is identical to the inelastic stress conjugate to  $\mathbf{D}_P$ , which follows from an assumption of internal equilibrium of the type suggested by the simple model in Fig. 5.

Finally, as the *third fundamental postulate*, we assume that the system is strongly dissipative such that  $\mathbf{T}$  and  $\mathbf{D}_P$  are related by dual inelastic potentials. *Viscoelasticity* follows and yields a nonlinear form of the Maxwell fluid (3).

*Plasticity*, as defined by rate-independent stress, represents a singular exception to the above: the magnitude  $|\mathbf{D}_P|$  becomes indeterminate. The assumption of overall independence of rate and history implies a relation of the form

$$|\mathbf{D}_P| = |\mathbf{D}|\vartheta(\mathbf{T}, \hat{\mathbf{D}}),$$

where  $\hat{\mathbf{D}} = \mathbf{D}/|\mathbf{D}|$ , and, hence, to a generalized form of *isotropic hypoplasticity*,

$$\overset{\circ}{\mathbf{T}} = \boldsymbol{\mu}_H(\mathbf{T}, \hat{\mathbf{D}}) : \mathbf{D}, \quad (7)$$

with a formula for  $\boldsymbol{\mu}_H$  in terms of the “inelastic clock” function  $\vartheta$ . In the standard theory of hypoplasticity,  $\vartheta(\mathbf{T}, \hat{\mathbf{D}})$  is independent of  $\hat{\mathbf{D}}$ , there is no distinction between elastic and plastic deformation rates, and the constitutive equation reduces to (7) with hypoplastic modulus taking the form

$$\boldsymbol{\mu}_H = \boldsymbol{\mu}_E(\mathbf{T}) - \mathbf{K}(\mathbf{T}) \otimes \hat{\mathbf{D}}, \quad (8)$$

where  $\mathbf{A} \otimes \mathbf{B} \hat{=} [A_{ij}B_{kl}]$ . Such models are popular with many in the granular mechanics community, particularly those interested in geomechanics, mainly because these models do not rely directly on the concept of a yield surface or inelastic potentials (whence the qualifier “hypo”),

although they do involve limit states where Jaumann stress rate vanishes asymptotically under the action of a constant deformation rate  $\mathbf{D}$ . This asymptotic state may be identified with the so-called “critical state” of soil mechanics, where granular dilatancy vanishes and the granular material flows essentially as an incompressible liquid.

The problem with the general form (8) is that it is exceedingly difficult to establish mathematical restrictions that will guarantee its thermodynamically admissibility, e.g., such that steady periodic cycles of deformation do not give positive work output. By contrast, models built up from elastic and dissipative potentials are much more likely to be satisfactory in that regard.

The treatise by Kolymbas provides an excellent overview and history of hypoplastic modeling.

### Anisotropy, internal variables and parametric hypoplasticity

Initially isotropic granular masses exhibit flow-induced anisotropy, particularly in quasi-static elastoplastic flow, since the grain kinetic energy or “temperature” is insufficient to randomize granular microstructure. This anisotropy is often modeled by an assumed dependence of elastic and inelastic potentials, and associated moduli, on a symmetric second-rank *fabric tensor*,  $\mathbf{A} \doteq [A_{ij}]$ , which is subject to a rate-independent evolution equation of the form

$$\overset{\circ}{\mathbf{A}} = \boldsymbol{\alpha}(\mathbf{T}, \hat{\mathbf{D}}, \mathbf{A}) : \mathbf{D}.$$

This represents a special case of the “isotropic extension” of anisotropic constitutive relations, where the anisotropic dependence on stress  $\mathbf{T}$  or strain  $\mathbf{E}$  is achieved by the introduction of a set of “structural tensors”, consisting in the simplest case of a set of second rank tensors and vectors. The structural tensors represent in turn a special case of a set  $\mathcal{X}$  of evolutionary internal variables consisting of scalars, vectors and second-order tensors.

At present, the origins of the evolution equations are unclear, although there may be a possibility of obtaining them from a generalized balance of *internal forces* derived on elastic and inelastic potentials which depend on the internal variables or their rate of change.

Whatever the origin of their evolution equations, it is easy to see that one can enlarge the set of dependent variables from  $\mathbf{T}$  to  $\{\mathbf{T}, \mathcal{X}\}$  with the evolution equations leading to *parametric hypoplasticity* defined by a generalization of (7). This gives a set of LODEs which describe the effects of initial anisotropy, density or volume fraction, etc., represented as initial conditions, and their subsequent evolution under flow. This formulation includes most of the current non-polar models of the evolutionary plasticity of granular media.

### Multipolar effects

In strongly inhomogeneous systems, such as the shear field associated with shear bands, we expect to encounter departures from the response of a classical simple (non-polar) material having no intrinsic length scale. The situation is generally characterized by non-negligible magnitudes of a Knudsen number  $K = \ell/L$ , where  $\ell$  is a characteristic microscale and  $L$  is a characteristic macroscale.

In the case of elastoplasticity, various empirical models suggest taking  $\ell$  to be about five to ten times the median grain diameter, a scale is most plausibly associated with the length of the ubiquitous *force chains* in static granular assemblies. These are chain-like structures in which the contact forces are larger than the mean force, and it is now generally accepted that these represent the microscopic force network that supports granular shear stress and rapidly reorganize under a change of directional loading. The micromechanics determining the length of force chains is still poorly understood.

Whatever the physical origins, a microscopic length scale serves as a parameter in various *enhanced continuum* models, including various *micropolar* and *higher-gradient* models, all of which represent a form of *weak non-locality* referred to by the blanket term *multipolar*. Perhaps the simplest is the Cosserat model, often referred to as *micropolar*. This model owes its origins to a highly influential treatise on structured continua by the Cosserat brothers, Eugène and François, celebrated internationally in 2009 on the occasion of the centenary of its original publication. Tejchman’s book provides a comprehensive summary

of a fairly general form of Cosserat hypoplasticity.

### Particle migration and size-segregation.

Another fascinating aspect of granular mechanics is the shear-driven separation or “unmixing” of large particles from an initially uniform mixture of large and small particles. Various models of particle migration in fluid-particle suspensions or size-segregation in granular media involve diffusion-like terms that suggest multipolar effects. While some models involve gravitationally driven sedimentation opposed by diffusional remixing, other models involve a direct effect of gradients in shearing akin to those found in fluid-particle suspensions.

It may be significant that many granular size-segregation effects are associated with dense flow in thin layers, which again suggests the likelihood of Knudsen-number or multipolar effects. Whatever the origins of particle migration, it can probably be treated as a strictly dissipative process, implying that it can be represented as a generalized velocity in a dissipation potential, thus suggesting a convenient way of formulating properly invariant constitutive relations.

### Relevance to material instability

There is a bewildering variety of instabilities in granular flow. These range from the shear-banding instabilities in quasi-static flow discussed above to gravitational layering in moderately-dense rapid flow and clustering instabilities in granular gases.

The author advocates a distinction between material or constitutive instability, representing the instability of homogeneous states in the absence of boundary influences, and the dynamical or geometric instability that occurs in materially stable media, such as elastic buckling and inertial instability of viscous flows. With this distinction, it is easier to assess the importance of multipolar and other effects.

Past studies reveal multipolar effects on elastoplastic instability, not only on post-bifurcation features such as the width of shear bands, but also on the material instability itself. This represents an interesting and challenging area for further research based on the parametric viscoelas-

tic or hypoplastic models of the type discussed above. The general question is whether and how the length scales that lend dimensions to subsequent patterned states enter into the initial instability leading to those patterns.

### Further Reading

1. Forterre Y., and O. Pouliquen. 2008, Flows of dense granular media. *Annual Review of Fluid Mechanics* 40:1–24.
2. Goddard, J. 2014. Continuum modeling of granular media. *Applied Mechanics Reviews*, submitted.
3. Kolymbas, D. 2000. *Introduction to Hypoplasticity*. Rotterdam: A. A. Balkema.
4. Lubarda, V. A. 2002. *Elastoplasticity Theory*. Boca Raton: CRC Press.
5. Ottino, J. M. and D. V. Khakhar. 2000. Mixing and segregation of granular materials. *Annual Review of Fluid Mechanics* 32:55–91.
6. Rao, K. and P. Nott. 2008. *An Introduction to Granular Flow*. Cambridge: Cambridge University Press.
7. Tejchman, J. 2008. *Shear Localization in Granular Bodies with Micro-polar Hypoplasticity*. Berlin: Springer.

**Biography of contributor**

Joe Goddard received his Ph.D. in chemical engineering from the University of California, Berkeley in 1962. He joined the chemical engineering faculty of the University of Michigan in 1963, and in 1976 he accepted a position in the Department of Chemical Engineering of the University of Southern California. He has been Professor of Applied Mechanics and Engineering Science in the University of California, San Diego, since 1991. His professional distinctions include NATO, NSF and Fulbright Postdoctoral and Senior Postdoctoral Fellowships, Fluor Professor of Chemical Engineering, University of Southern California, D.L. Katz Lecturer, University of Michigan, President, U.S. Society of Rheology, G.I. Taylor Medalist of the Society of Engineering Science, and visiting scholar and researcher at several universities in Europe and the U.S., including a visit as Springer Visiting Professor in the University of California, Berkeley.